Coastal Dynamics 2009
Paper No.

MODELING SEDIMENT TRANSPORT AND DELTA MORPHOLOGY ON THE DAMMED ELWHA RIVER, WASHINGTON STATE, USA

Guy Gelfenbaum[1], Andrew Stevens[2], Edwin Elias[3], and Jonathan Warrick[4]

Abstract

The sediment supply to the delta and adjacent beaches of the Elwha River in Washington State, USA is expected to increase significantly after removal of two dams. This paper describes the initial implementation of a process-based hydrodynamic and sediment transport model to predict sediment transport pathways and delta morphological response to changes in sediment supply in a mixed sediment system. The hydrodynamic model is calibrated and validated against water levels and currents measured in the Strait of Juan de Fuca and on the Elwha delta. Strong instantaneous and residual tidal currents are responsible for the transport and dispersal of fine-grained and sand-sized sediments across the delta. If sediment supply is large enough, some sediment will accumulate on the delta, modifying the delta substrate, which is presently dominated by hardbottom and coarse sediments.

Key words: Elwha River, sediment transport, morphodynamics, sediment supply, delta morphology, dammed river

1. Introduction

The geomorphology of a river delta is determined by a balance among river-supplied sediment, relative sea level, and coastal processes, including waves and tides. Changes in any one of these forcings will alter the distribution of sediment and resulting delta morphology. A common anthropogenic influence on deltas arises from reducing sediment supply by the damming of coastal rivers. Dams within coastal watersheds can reduce sediment supply to the coast, resulting in shoreline erosion as well as modification of delta and nearshore habitats. Well-documented examples of shoreline modifications resulting from reduced sediment supply on a dammed river system include the Ebro Delta in Spain (Jimenez, et al., 1997) and the Nile Delta in Egypt (Frihy et al., 2008).

To study the effects of changing sediment supply on delta morphology in a mixed grain size sediment system we examine the Elwha River delta in northern Washington State, USA (Figure 1). The Elwha system is ideal because 1) two dams significantly reduce sediment supply to the delta (Randle et al., 1996), 2) there is a wide range of sediment sizes on the beaches of the delta and trapped behind the dams, and 3) both dams will be removed in the near future. The removal of the two dams and subsequent availability of at least a portion of the sediment that had been trapped behind the dams will provide a large-scale 'experiment' to test predictions of the morphologic response to an increase in sediment supply. It is hypothesized that sediment transport pathways, as well as areas of deposition will vary on the delta for the different grain-size classes delivered by the river (Figure 2), possibly resulting in changes to substrate and habitats around the delta. Herein we describe progress toward implementation of a process-based hydrodynamic and sediment transport model that can predict short- and long-term sediment transport pathways and delta morphological response to changes in sediment supply in a mixed sediment system. Initial model simulations combined with field data are used to evaluate the relative importance of different forcing mechanisms on transport of coarse- and fine-grained sediment on the delta.

[1] U.S. Geological Survey, 345 Middlefield Rd., Menlo Park, CA 94025, USA. ggelfenbaum@usgs.gov
[2] U.S. Geological Survey, 345 Middlefield Rd., Menlo Park, CA 94025, USA. astevens@usgs.gov
[3] Deltares, 345 Middlefield Rd., Menlo Park, CA 94025, USA. eelias@usgs.gov
[4] U.S. Geological Survey, 400 Natural Bridges Dr., Santa Cruz, CA 95060, USA. jwarrick@usgs.gov

2. Setting

The Elwha River drains approximately 800 km^2 of the Olympic Mountains of Washington State, and empties into the Strait of Juan de Fuca, the entranceway to Puget Sound (Figure 1). Early in the last century two dams were constructed on the Elwha River for hydroelectric power generation. The 33-m tall Elwha Dam was built 8 km from the river mouth in 1910-1913 and the 64-m tall Glines Canyon Dam was built 21 km from the mouth in 1925-1927 (Duda et al., 2008). Operation of the dams has been primarily as run-of-the-river, a common practice in which the amount of water entering the reservoirs is simultaneously released through the dam. While this method minimizes alteration of the flow regime downriver, sediment is still trapped behind the dams when the river-bearing load is deposited as the river slows upon entering the reservoir.

Figure 1. Location map of the Elwha River emptying into the Strait of Juan de Fuca in Washington State, USA

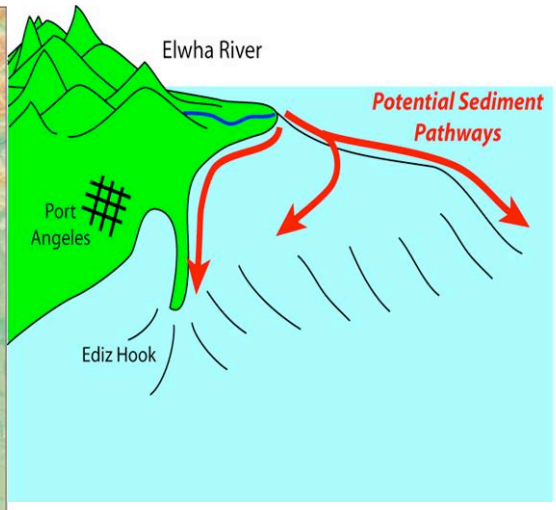

Figure 2. Conceptual model of potential pathways for sediment after dam removal. View looking from the NE

River discharge peaks in winter due to heavy rain and again in late spring due to snowmelt (Duda et al., 2008). Based on USGS gauging station measurements at river km 13.8 the annual average discharge is 42 m^3/s, the minimum average monthly discharge is about 20 m^3/s during September and the peak monthly mean discharge is about 64 m^3/s during spring snowmelt (Curran et al., in press). This decade has included two of the largest discharge events on record, with a rainfall-induced peak instantaneous discharge in 2006 of 592 m^3/s and a peak instantaneous discharge in 2007 of 990 m^3/s.

Field surveys estimate that the reservoirs behind the two dams trapped 13.5 million m^3 of sediment, and the present-day total may be closer to 15 million m^3. The sediment that accumulated behind the dams is composed of 52% silt and clay, 35% sand, and 13% gravel and cobble (Gilbert and Link, 1995). Randle et al. (1996) suggest that about 5 million m^3 of sediment may be mobilized and transported down the river to the Strait within the first 3 years after dam removal. The amount of sediment mobilized and transported downstream will depend on the number, intensity, and duration of high flow discharge events.

The Elwha River delta is comprised of sub-aerial and sub-marine morphologic components, each of which is characterized by a nearly symmetrical protrusion into the Strait of Juan de Fuca (Figure 3). The shoreline and sub-aerial delta configuration is mimicked by a similarly-shaped but larger submarine delta, with a slope break at about 50-60 m water depth. The lower river floodplain has been modified by a pair of flood-control dikes and the channel is less mobile and winnowed of sands as compared to a control reach upstream of the dams (Draut, et al., 2008), likely as a result of the dams preventing sand-sized material from passing to the lower river.

Beaches along the Elwha River delta are mixed sand and gravel. Analysis of aerial photographs show that the delta experienced net erosion between 1939 and the 1990s (Schwartz and Johannessen, 1997). Shoreline erosion rates on the delta appear to have increased from 0.3 m/yr during 1936-1990 to 1.7 m/yr during 1990-2006 to 2.8 m/y during 2004-2006 suggesting a greater impact from the reduced sediment supply to the delta (Warrick et al., in press). Beaches west of the river mouth are generally steep and reflective and have been relatively stable over the last several years (Warrick et al., in press). East of the river mouth the beaches have a steep upper foreshore and a flatter, more dissipative low-tide terrace. Beaches east of the river mouth have been regularly eroding, exposing more and more of the low-tide terrace, which is a coarse cobble and boulder lag. The Elwha River delta fits within a littoral cell that is 11.8 km long and bounded by a bedrock headland at the west end of Freshwater Bay on the west and the end of Ediz Hook to the east (Wallace, 1988). Net shore drift is from west to east as evidenced by the shoreline morphology and development of Ediz Hook, a long spit protecting the city of Port Angeles (Figure 3). Wallace (1988) estimated a net shore drift to the east of about 9000 m^3/yr.

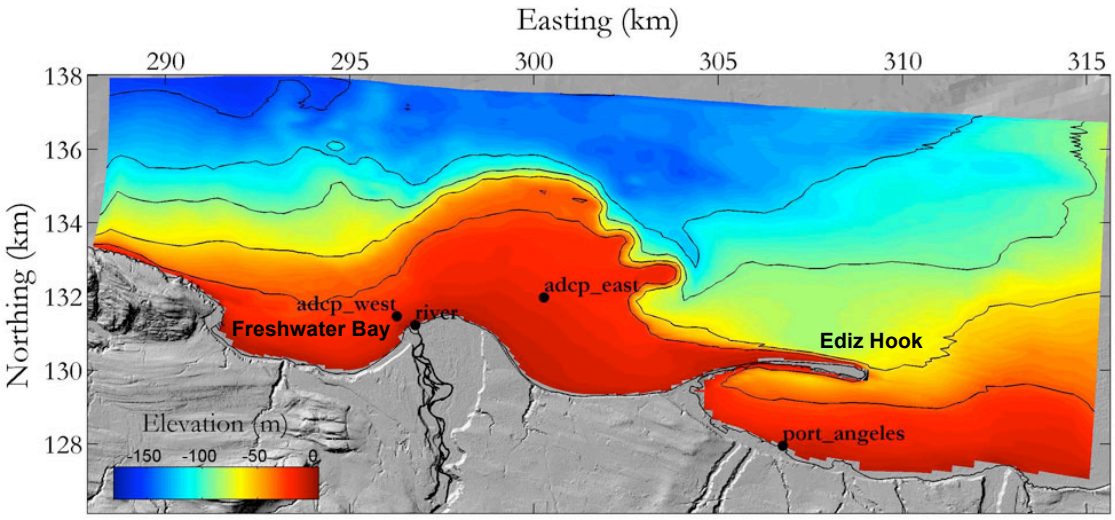

Figure 3. Map of Elwha River delta as it protrudes into the Strait of Juan de Fuca. Adcp_west and Adcp_east identify the locations of the instrument-mounted frames that measured waves and currents.

Substrate type and distribution across the submarine portion of the delta was characterized by combined sonar and underwater video mapping (Warrick et al., 2008). The sonar mapping covered the western portion of the submarine delta out to about 40-m water depth, however only a small portion of the eastern delta has thus far been mapped. Four main substrate types are identified: sand, mixed gravel and cobbles, hard (boulders and bedrock), and sand waves. Mud was not identified in any significant proportion. The substrate is generally coarser on the western side of the delta, whereas there is more sand near the central part of the delta near the river mouth (Warrick et al., 2008). In general, the substrate distribution is highly heterogeneous. Warrick et al. (2008) also discussed the mapping of kelp, which prefers hard substrates. With an abundance of kelp, hard substrates including bedrock and boulders, sandwave fields, and the lack of any mud, Warrick et al. (2008) speculate that the sediment transport from waves and tidal currents exceeds the input of fine sediment from the river. Of significant concern to local managers is whether the removal of the dams will lead to an increase in the supply of fine sediment that will exceed the sediment transport on the delta, resulting in a change of the substrate and the delta ecosystem. This paper will start to explore this question through the synthesis of field observations and the implementation of process-based hydrodynamic and sediment transport model for the Elwha River delta.

3. Hydrodynamic and Sediment Transport Model

We have implemented a spatially explicit, process-based hydrodynamic and sediment transport model

using Delft3D for the Strait of Juan de Fuca, with increased spatial resolution in the vicinity of the Elwha River delta (Figure 4). The flow module of Delft3D solves the unsteady shallow-water equations on a structured curvilinear grid subjected to tidal and meteorological forcing. Waves are modeled using the 3rd generation SWAN processor and are solved at 60-minute intervals. Waves and currents are coupled to include the effects of the waves on the currents (e.g., enhanced bed shear stresses and the generation of longshore currents due to wave breaking) and the effect of the currents on the waves (e.g., wave steepening when the wave propagation direction opposes the currents) (Walstra et al., 2000). Sediment transport is calculated following van Rijn (1993). Sediment transport and morphological bed updating are calculated at each computational time step. Testing and validation of the basic sediment transport and morphology updating model are reported in Lesser et al. (2004).

To derive accurate boundary conditions, the Elwha model is nested in a larger scale hydrodynamic model that includes the Strait of Juan de Fuca, Georgia Basin, and Puget Sound. The large-scale hydrodynamic model is forced with tidal boundary conditions where the Pacific Ocean meets the Strait. Wave forcing includes both swell entering from the Pacific Ocean and locally-generated wind waves.

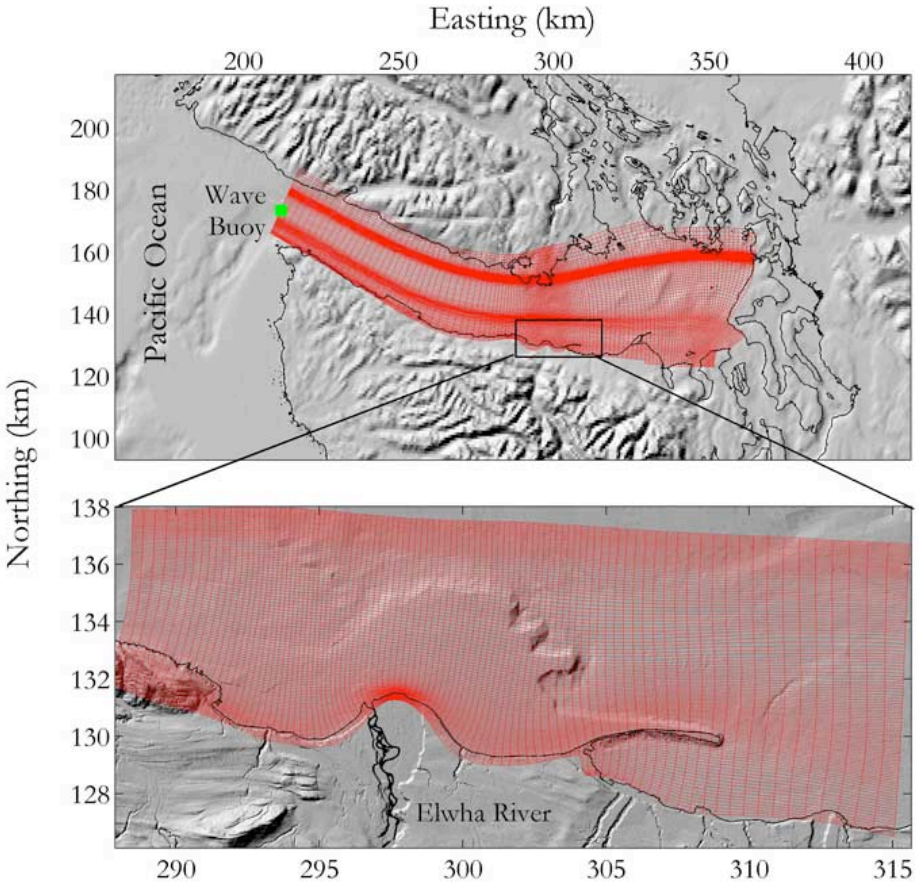

Figure 4. Curvilinear grid for the wave and flow models for the Strait of Juan de Fuca (above) and a high-resolution grid for the region around the Elwha River delta (below).

3.1 Field data and model calibration/verification

The large-scale flow model is calibrated and verified against NOAA predicted water levels at several stations throughout the Strait, Georgia Basin, and Puget Sound. Currents, water levels, and wave data collected at two sites on the delta were used to validate the high-resolution Elwha model. During the spring of 2005 and the winter of 2006, two instrumented frames were deployed near the 18-m contour, one east of the delta center and the other west of the delta center, just offshore of the river mouth (Figure 3). Mounted on specially-built low-lying frames were upward-looking 1200 kHz ADCPs programmed to

measure waves every hour (at 2 hz during 20 min bursts) and current profiles every 15 min. Current measurements were obtained at 0.75-m intervals from 1.8-m above the bottom to the water surface. Pressure sensors on the ADCPs provided water levels every 15 min at both sites.

3.1.1 Water levels and currents

Tides in the Strait of Juan de Fuca are mixed semi-diurnal with a strong spring-neap variation (Figure 5, top panel) and a 1.4-m mean tidal range (at NOAA Tide Station Port Angeles). Strong currents over 1 m/s are observed on both sides of the Elwha River delta. Currents along the delta are dominated by tidal forcing, with tidal harmonics accounting for 90% of the variance of the depth-averaged currents at both stations. The dominant orientation of the currents varies across the delta, with currents oriented northeast-southwest on the west side and northwest-southeast on the east side of the delta (Figure 5, bottom panel). Tidal currents are stronger on the east side than on the west side.

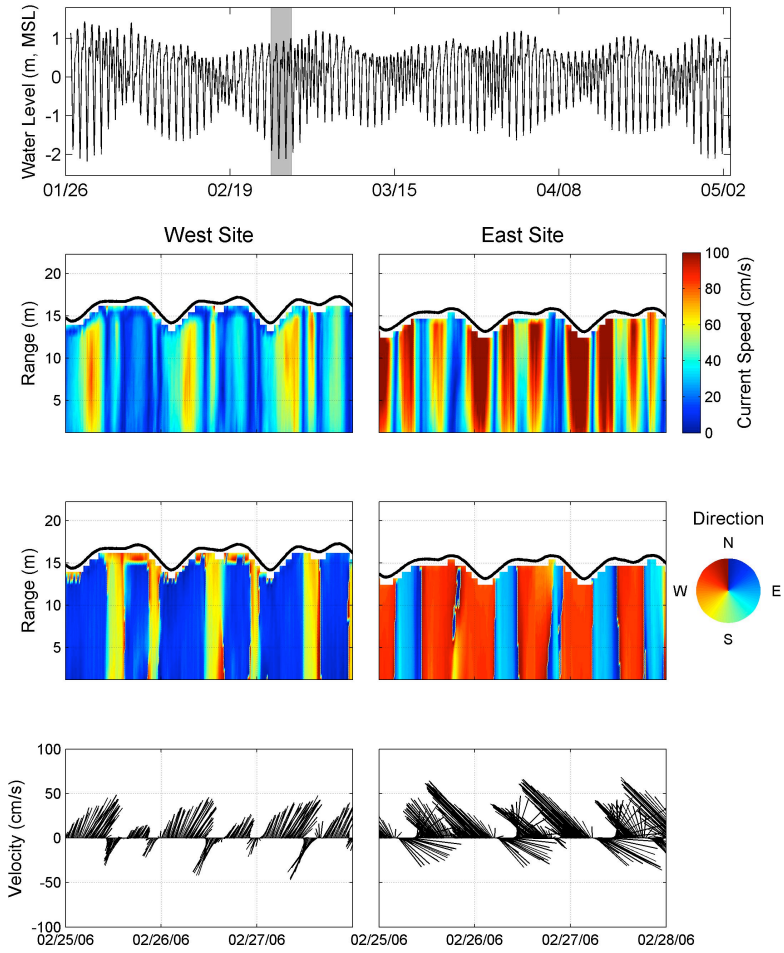

Figure 5. Water level from Jan 26 – May 2, 2006 (top panel), and current speed, current direction, and depth-averaged current vectors at West and East sites during a spring tide from Feb 25-28, 2006 (bottom three panels)..

For the hydrodynamic model, tidal constituents were adjusted at the sea boundary to minimize the differences between modeled water level amplitude and phase and those reported at NOAA tide stations across the Strait of Juan de Fuca. At the two measurement sites on the Elwha delta, water-level amplitude and phase for the five main tidal constituents (O_1, K_1, N_2, M_2, and S_2) compare well between model and data, with a total RMS error of about 0.12 m at each measurement site (Figure 6). Depth-averaged currents at the two sites, when decomposed into harmonic constituents, also compare well (Table 1 and 2; Figure 7). A Chezy bed roughness parameterization with a constant value of 60 was used across the entire model domain. Although tidal current predictions at the two measurement sites may be improved slightly with a

varying bottom roughness, insufficient data exists to warrant a spatially-varying roughness.

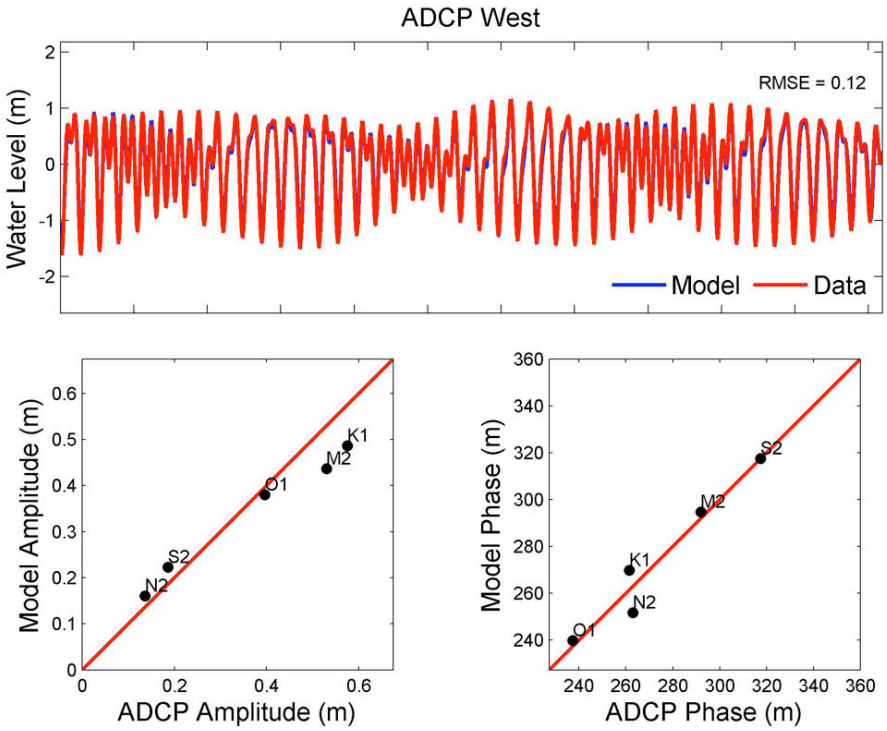

Figure 6. Water level amplitude time series comparison between model (blue) and data (red) (top panel), and modeled versus measured amplitude and phase for each of the 5 major tidal constituents (bottom two panels)..

Table 1. Comparison of modeled and measured major axis depth-averaged current amplitude, orientation, and phase for each tidal constituent at the West Site

Constituent	Major Axis Amplitude (m/s)		Orientation (deg.)		Phase (deg.)	
	Model	Data	Model	Data	Model	Data
O1	0.12	0.11	42.2	45.9	103.9	96.7
K1	0.11	0.12	41.7	46.8	124.1	106.6
N2	0.05	0.06	43.7	50.6	176.0	194.8
M2	0.24	0.23	41.0	49.4	241.5	231.7
S2	0.07	0.07	39.6	47.1	246.3	247.0

Table 2. Comparison of modeled and measured major axis depth-averaged current amplitude, orientation, and phase for each tidal constituent at the East Site

Constituent	Major Axis Amplitude (m/s)		Orientation (deg.)		Phase (deg.)	
	Model	Data	Model	Data	Model	Data
O1	0.16	0.15	172.7	172.5	321.4	327.4
K1	0.23	0.26	163.2	164.1	347.6	354.7
N2	0.16	0.15	154.8	157.1	42.1	49.6
M2	0.80	0.69	157.4	157.1	97.0	89.7
S2	0.24	0.22	159.0	157.9	105.9	120.3

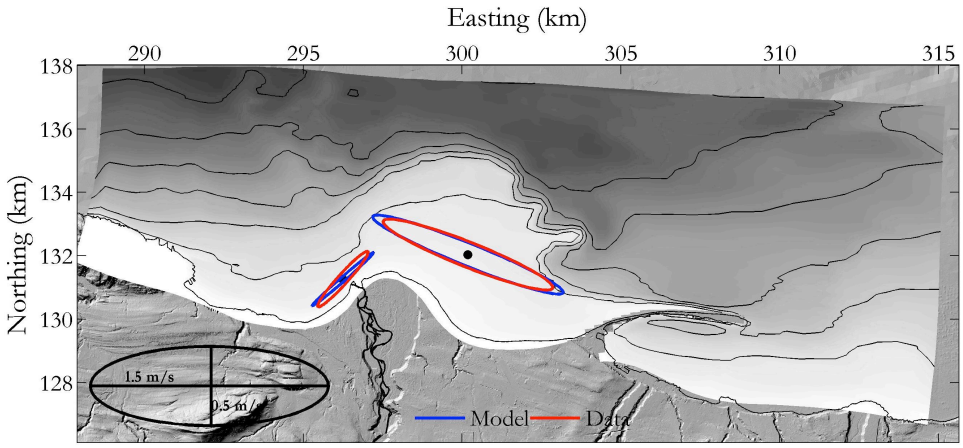

Figure 7. Depth-averaged current ellipses showing model (blue) and data (red) at two locations on either side of the delta.

Residual currents are large and the patterns are complex around the delta (Figure 8). Residual currents up to 40 cm/s are oriented eastward and northward offshore of the delta center. Strong residual currents, up to 30 cm/s, extend all the way across the delta. A residual eddy rotating clockwise forms on the east side of the delta with currents between 10-20 cm/s and a smaller eddy exists on the west side of the delta. Model predictions match the measured residual currents at the two measurement sites in magnitude but are slightly off in direction (Figure 8).

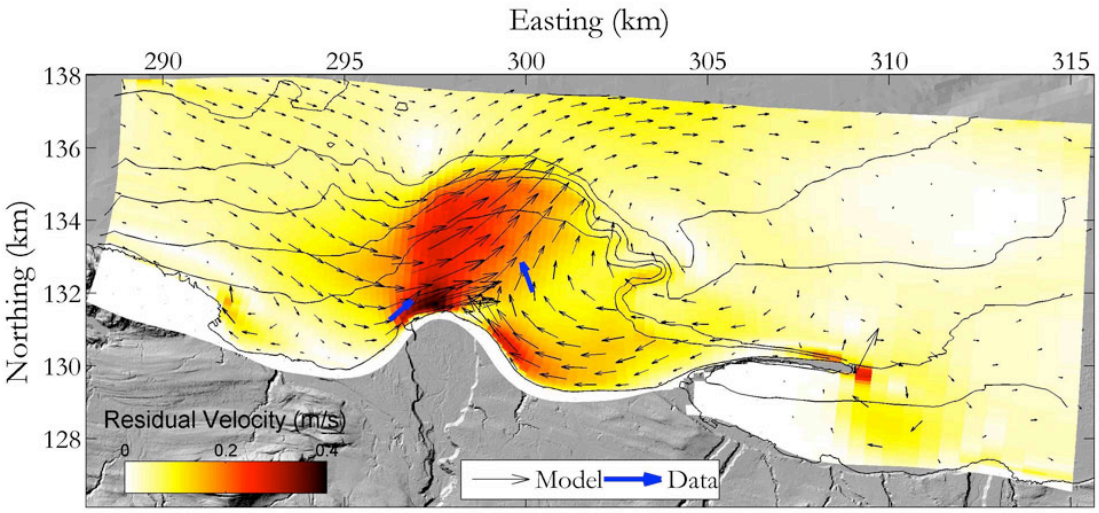

Figure 8. Map of modeled depth-averaged residual currents and the measured residual currents (blue) at the two measurement sites on either side of the delta.

3.1.2 Waves

Wave data were obtained from NOAA Buoy 46087 located at the entrance to the Strait (Figure 4) and from the two measurement sites on the delta. In general, waves reaching the delta are generated predominately from swell traveling down the Strait from the Pacific Ocean and secondarily from locally-generated winds (Figure 9). Swell, with wave periods between 9-12 s (0.11-0.08 hz), occurred about 90% of the time during the winter deployment. Wind waves, with periods less than about 5 s, also came from the east (e.g., day 47 in Figure 9).

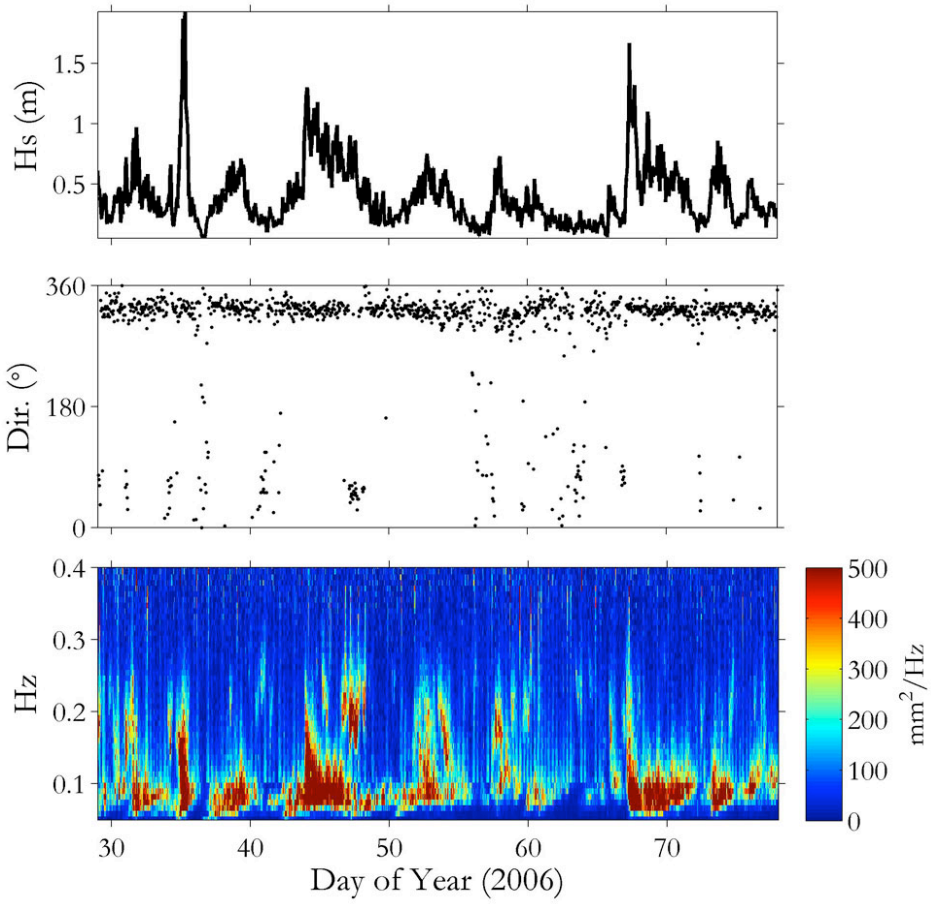

Figure 9. Time series of significant wave height (top panel), direction (middle panel), and 2D wave spectra (bottom panel) for about 2 months in winter 2006 at the East Site..

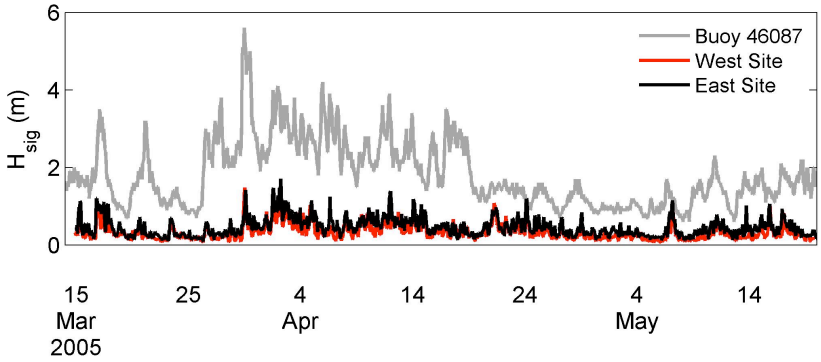

Figure 10. Time series of significant wave height at NOAA Buoy 46087at the entrance to the Strait (gray) and at the two measurement sites, west (red) and east (black).

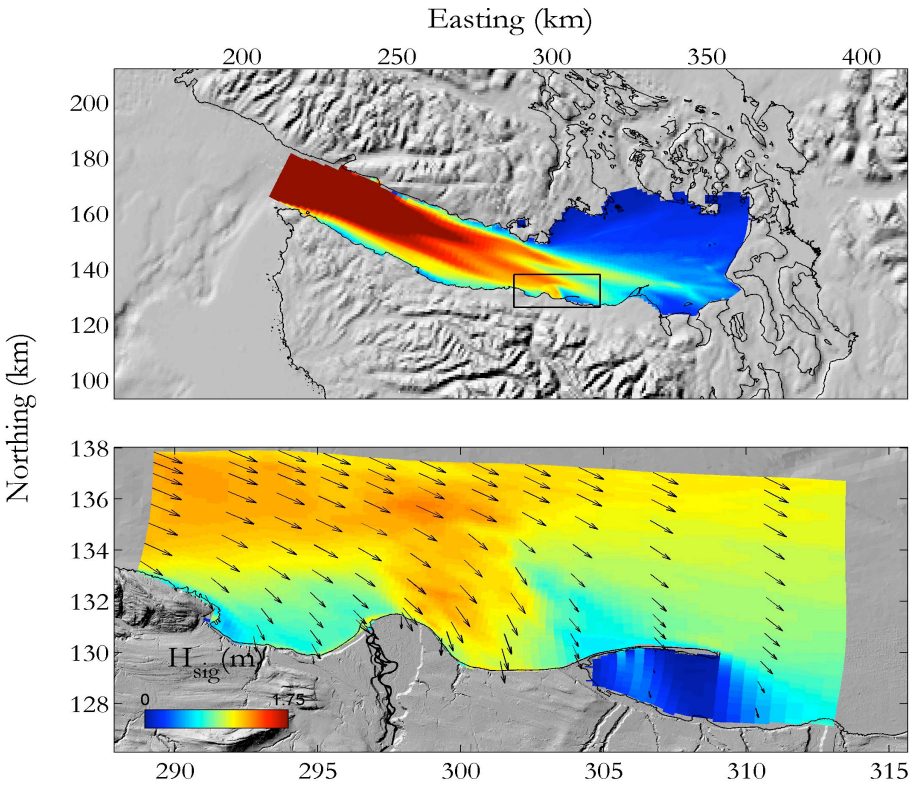

Figure 11. Map of modeled significant wave height initiated with a 5.8-m wave at the entrance to the Strait (top panel) and expanded to show variations in wave height and direction around the delta (bottom panel).

Wave energy is dissipated traveling along the Strait with significant wave heights decreasing from the entrance of the Strait to the Elwha delta by an average of 20-30% and a maximum during large waves of about 60% (Figure 10). The pattern of wave height decay across the Strait is not uniform (Figure 11, top panel) and the pattern of wave heights across the delta is highly dependent on the tide as wave-current interactions are important (Figure 11, bottom panel). The west side of Freshwater Bay is relatively protected from ocean swell as compared to the delta. More importantly, wave direction and impact angle along the coast is significantly different on both sides of the delta. On the west side, the waves approach more perpendicular to the coast orientation, resulting in smaller longshore drift rates, beach cusps, and a higher berm elevation (Warrick et al., in press). On the central and eastern side of the delta, wave direction is more oblique to the orientation of the shoreline, resulting in greater longshore drift rates. These findings are consistent with the recent field observations of longshore transport rates using radio-tagged cobbles at different locations around the delta (I. Miller, personal communication).

3.2 Morphodynamic model approach

The hydrodynamic and sediment transport model is used in a number of ways to elucidate the sediment transport pathways and depositional patterns associated with changing Elwha River sediment supply to the delta. One approach is to operate the model in 3D to capture buoyant river-plume dynamics and dispersal of fine-grained sediments. Running the model in 3D, with 10 layers in the vertical, is computationally more expensive yet is required to fully capture the freshwater plume dynamics and fine-sediment dispersal. The second approach is to operate the model in 2D depth-averaged mode to simulate wave and tidal processes driving transport of sand-sized sediment on the delta. The model is forced with a time series of wind and waves and tidal harmonics on the boundary for several weeks to months, or it is forced with one or more wave classes to simulate a particular wave event.

A third approach is to operate the model 'scaled up' to simulate long-term morphological responses to changing sediment supply. This long-term modeling uses a representative wave climatology (deVriend et

al., 1993) (Table 3), and a morphological acceleration factor or MORFAC (Lesser et al., 2004). Long-term morphological simulations with the Elwha model represent up to one year of actual transport. A wave climatology composed of four wave classes representing swell from the Pacific Ocean was developed from analysis of data from wave buoy 46087. For each wave class, a Strait of Juan de Fuca model was run for 2 weeks to average the effects of wave-current interactions and the mean wave statistics were prescribed at the boundaries of the nested high-resolution Elwha model (Table 3). Two additional wave classes were added to the climatology to represent locally-generated wind waves coming from the east.

Table 3. Schematized wave climate

Wave Class	Significant Wave Height (m)	Peak Wave Period (s)	Wave Direction (°T)	Percent Occurrence (%)	Run Time (days)	MORFAC
1	0.36	9.0	294	31	5.2	21.9
2	0.62	9.9	294	49	10.3	17.3
3	0.85	11.2	294	9	2.6	12.7
4	1.12	11.7	294	1	2.6	1.4
5	0.2	5.0	40	8	5.2	5.6
6	0.7	6.0	45	2	2.6	2.8

4. Results

4.1 Sediment supply

Sediment supply from the river to the Strait is not known because it has not been measured below the dams. However, annual surveys of nearshore bathymetry and beach topography using RTK DGPS since 2004 (Warrick et al., 2007) provides a glimpse into the supply of sediment from the river under high discharge events. Detailed surveys collected in September 2007 and again in September 2008 reveal an accumulation of approximately 34,000 m^3 of sediment directly off the mouth of the river (Figure 12). This sediment accumulation is likely associated with the peak discharge event from the intervening December 2007 flood.

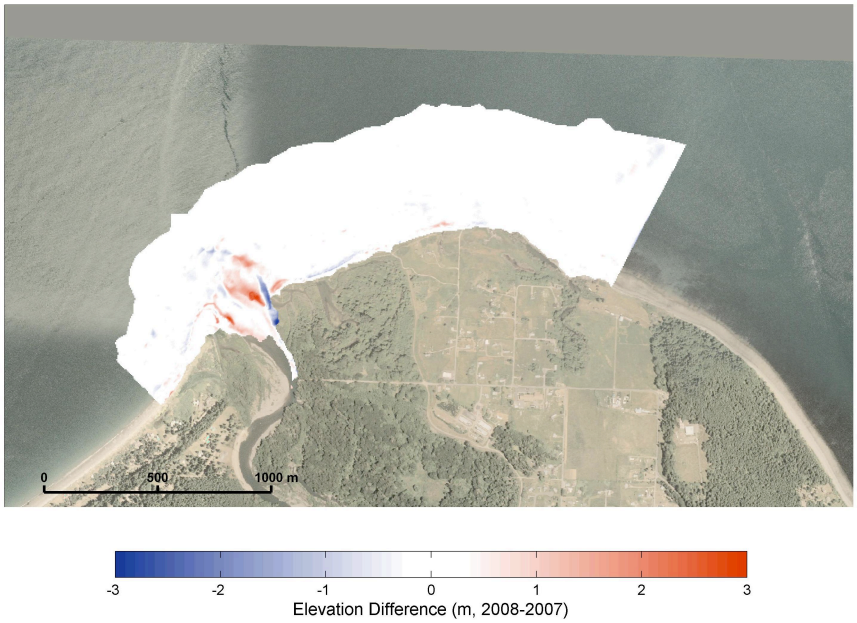

Figure 12. Map of measured sediment accumulation and erosion calculated as a difference between the beach topography and delta bathymetry measured in 2008 and 2007.

The deposition event associated with the 2007 river flood shows the magnitude and location of sediment accumulation off the river mouth under sediment-limited conditions, i.e., with the dams in place limiting sediment transport down the river. After the dams are removed, the sediment supply from the river is likely to increase, especially during the first few years after dam removal. In this paper we will not attempt to predict the actual sediment load after dam removal, but for modeling purposes we will explore the impact of increasing the sediment supply by about an order of magnitude to 280,000 m^3 over the present dammed river condition.

4.2 Sediment transport

4.2.1 Littoral transport

The steep foreshores and narrow surf zones of Puget Sound and Strait of Juan de Fuca beaches result in littoral transport being dominated by swash processes at the waterline (Warrick et al., in press; Finlayson, 2006). Presently Delft3D does not incorporate swash processes into its formulation; therefore, the model in its present form is not appropriate for explicitly calculating littoral drift rates for the steep beaches and narrow surf zones of the Elwha delta. Instead, we follow Warrick et al. (in press) and use the formulations proposed by van Wellen et al. (2000) to estimate the longshore transport rates of sediment on the beaches of the delta.

Along a significant portion of the western side of the delta, both modeling and observations suggest that the swell waves generally approach the beach perpendicular to the shoreline orientation (Figures 11 and 13), and therefore will induce no net longshore sediment transport. These findings are consistent with initial results of longshore transport experiments using cobble tracers on the west-side beaches (I. Miller, personal communication). Along the east-side beaches, waves approach from a steep angle (Figures 11 and 13), inducing a significant longshore transport.

Estimates of the longshore transport rates on the foreshore along the eastern side of the delta vary between 10,000-200,000 m^3/yr, with the large range owing to the uncertainty in the coefficients for mixed and coarse sediments. These foreshore transport rates are likely 25-40 times greater than the transport rates on the low-tide terrace because of differences in mean grain size, bed slope, and percent of time impacted (Warrick et al., in press).

Figure 13. Photographs of waves breaking perpendicular to the beach on the west side of the delta (left panel) and at an oblique angle on the east side of the delta (right panel)..

4.2.2 Fine-grained transport

If suspended-sediment concentrations in the river become high enough after dam removal, hyperpycnal flows will form when the density of the sediment laden freshwater from the river becomes greater than the density of the seawater in the Strait (Mulder and Syvitski, 1995). Given that the adaptive management plan for the removal of the dams calls for the cessation of dam notching if concentrations become too high, we will only consider the lower sediment concentrations that induces buoyant plume transport. Under these conditions, the dispersal of fine-grained sediment will be highly influenced by the direction and magnitude of the tidal currents across the delta (Figure 14).

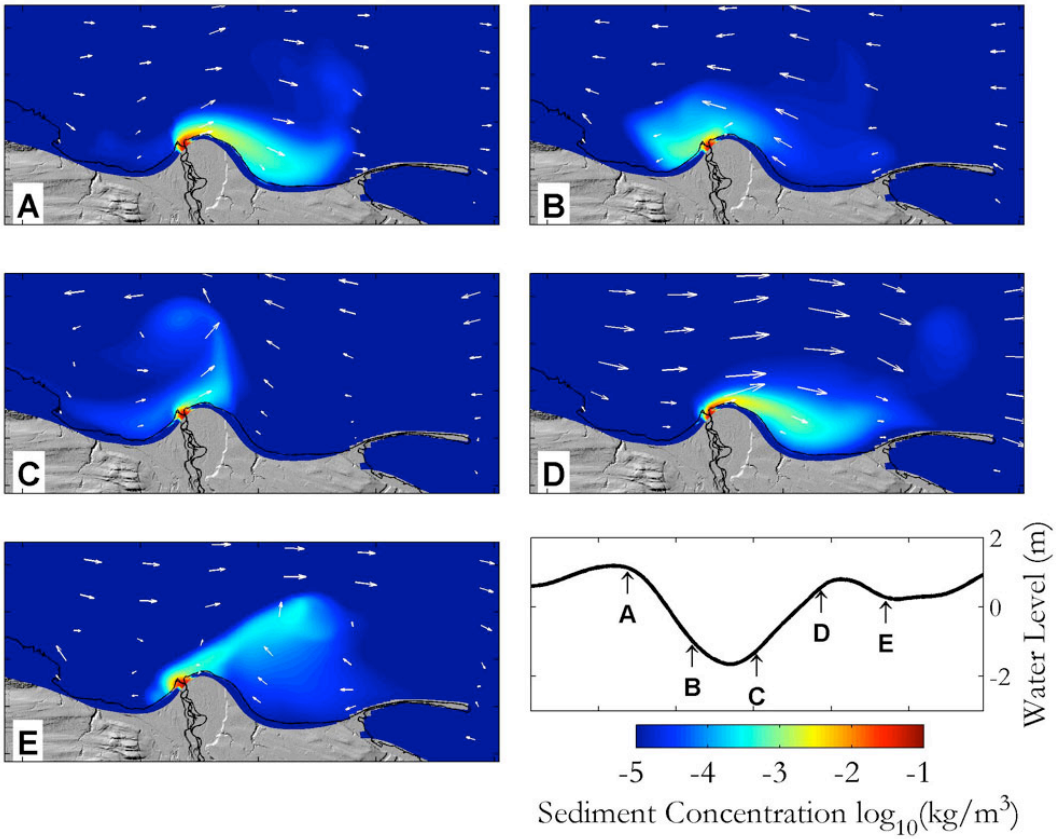

Figure 14. Maps of modeled sediment concentration and surface current vectors at various phases of the tide.

During ebbing tides (Figure 14 panel B), the buoyant plume and fine-grained sediment will be primarily dispersed to the west, though tidal currents along the west side of the delta are not as large as the tidal currents along the east side of the delta. Conversely, during flooding tides (panel D), the buoyant plume and fine-grained sediment will be dispersed to the east, and because the tidal currents are greater on the east side of the delta, the sediment is carried farther away from the river mouth. During the strong flood and ebb tides, the plume and suspended sediment are close to shore. As the tides switch from ebbing to flooding or from flooding to ebbing (panels C and E, respectively), the buoyant plume and suspended sediment get carried to the north, away from the coast and into deeper water.

4.2.3 Morphologic response

In order to understand the morphologic response to a hypothesized restored river sediment supply, a depth-averaged morphodynamic simulation for a one-year period was made. Model simulations suggest that a larger sediment supply, such as might be expected after dam removal, will deposit sediment off the river mouth, in a zone spread east and west by tidal currents (Figure 15). Owing to the asymmetry in the tidal currents off the river mouth, sand will be differentially deposited east of the river mouth in higher percentages and silt will be more evenly deposited west and east of the river mouth (Figure 15, lower panels). The weaker tidal currents directed to the west can transport the silt more readily than the sand, whereas the stronger currents to the east can transport both sizes. Thin accumulations of both sand and silt are predicted across most of the delta, with thicker accumulations found in deeper water off the east edge of the delta and east of Ediz Hook just inside of the harbor.

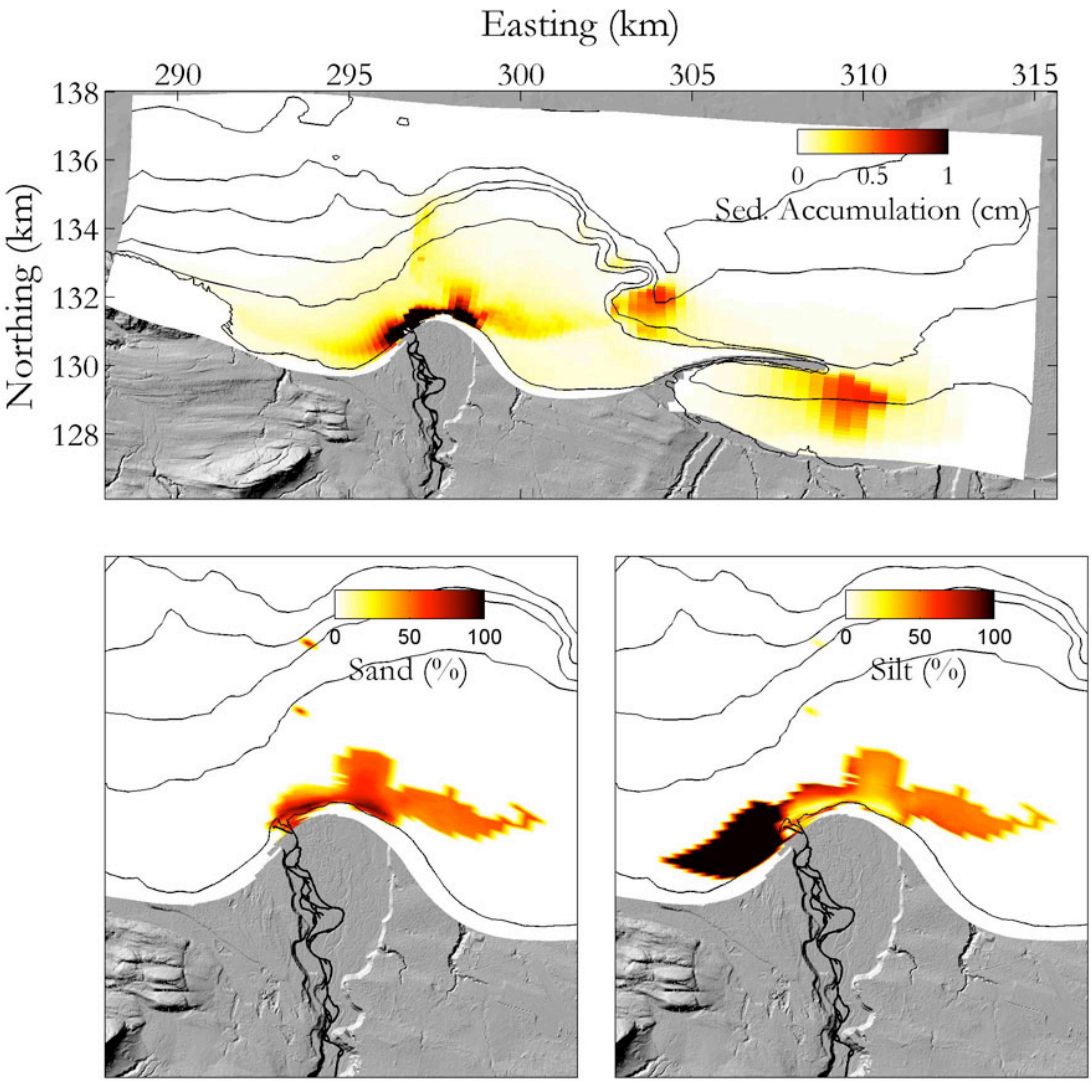

Figure 15. Map of modeled sediment accumulation after one year of morphological simulation for one condition of sediment supply (top) and zoomed in view of percent sediment accumulation for sand (bottom left) and silt (bottom right)

5. Conclusions

Over the last several decades, morphologic change of the Elwha delta has included the erosion and landward migration of the shoreline on the eastern side of the river mouth. The steep wave angle against the mixed grain-size beaches along the tip of the delta induce significant longshore transport potential. As sufficient sediment is not supplied by the river to balance the sediment lost to longshore transport, erosion of the shoreline occurs. There is also evidence that the substrate on the delta has coarsened, leaving more exposed hardbottom, cobbles, and boulders. This is likely owing to the reduction in supply of river sediment, especially the finer sediment. The harder substrate may have benefited certain species of algae, including the large Bull Kelp (Warrick et al., 2008) which is concentrated in bands on either side of the delta.

After dam removal on the Elwha River, sediment loads are expected to increase substantially, especially during flood events. The newly exposed sediment will consist of a wide range of sediment sizes which will be available to be transported down the river to the delta and beaches. A portion of the coarse

sediment (sands and gravels) will likely first deposit near the river mouth and become available to the beaches. These coarse sediments will then be acted on predominately by swell waves approaching from the west-northwest and transported alongshore to the east. The addition of this sediment to the longshore drift, starting at the river mouth, is likely to slow, if not stop, the shoreline erosion occurring on the central part of the delta.

Finer sediment (silts and sands) will enter the delta both within buoyant plumes and as accumulations on the delta adjacent to the river mouth. The finer sediment will be transported predominately east and west, but also northward away from the shoreline by tidal currents. Tidal current velocities are enhanced over the delta and form eddies on the downstream side of the delta with most tidal excursions. In addition to the large instantaneous tidal currents, tidal residual currents are very large. The centers of the tidal current eddies do not concentrate sediment accumulation on the bed, consistent with the findings of Signell and Harris (2000). Instead, if sediment supply is large enough, then sediment tends to accumulate in a band on either side of the river mouth. Some of the sediment leaves the delta and is deposited off the eastern edge of the delta and off the end of Ediz Hook.

The balance between sediment supply from the river and hydrodynamic processes on the delta controls the accumulation of sediment on the delta and will effect changes in substrate as well. The simulations presented here have demonstrated the utility of using numerical models of hydrodynamics and sediment transport to gain a better understanding of the morphologic response of deltas in mixed sediment environments to changing sediment supply. Additional simulations exploring various sediment supply rates, as well as other model parameters, including different wave climatologies, will likely result in additional insights into this complex system.

Acknowledgements

This work is funded by the U.S. Geological Survey, Coastal and Marine Geology Program. Thanks to Jeff Duda for his leadership in coordinating USGS research in support of the Elwha River Restoration project. Andrew Schwartz and several interns from Washington Department of Ecology collected the beach topography data. Joanne Thede Ferreira and Hal Williams assisted with the deployment and recovery of the current meters. We thank Matt Beirne and the Lower Elwha Klallam Tribe for allowing us access to the delta and Ian Miller, a University of California-Santa Cruz graduate student working with the USGS, who collected sediment transport data along the beaches of the Elwha delta using radio-tagged cobbles. Critical reviews from JingPing Xu and Alex Apotsos helped to improve this manuscript.

References

Curran, C.A.., Konrad, C.P, Higgins, J.H., and Bryant, M.K., in press, Measurements of sediment load prior to dam re moval in the Elwha River, Clallam County, Washington, U.S. Geological Survey Scientific Investigations Report.

De Vriend, H.J., Capobianco, M., Chesher, T., De Swart, H.E., Latteux, B. and Stive, M.J.F., 1993. Approaches to long-term modelling of coastal morphology: a review. *Coastal Engineering*, v. 21, p. 225-269.

Draut, A.E., Logan, J.B.,. McCoy, R.E., McHenry, M., and Warrick, J.A., 2008. Channel evolution on the lower Elwha River, Washington, 1939–2006. *USGS SIR 2008-5127.*

Duda, J.J., J.E. Freilich, and E.G. Schreiner, 2008. Baseline studies in the Elwha River ecosystem prior to dam removal: Introduction to the special issue. *Northwest Science*, v. 82, p. 1-12.

Finlayson, D., 2006. The geomorphology of Puget Sound beaches. Puget Sound Nearshore Partnership Report No. 200 6-02. Washington Sea Grant Program, University of Washington. Available at http://pugetsoundnearshore.org**.**

Frihy, O.E., S.M. Shereet, and M.M. El Banna, 2008. Pattern of beach erosion and scour depth along the Rosetta Promontory and their effect on the existing protection works, Nile Delta, Egypt. *Journal of Coastal Research*, v. 24, n. 4, p. 857-866.

Gilbert, J.D. and R.A. Link, 1995. Alluvium distribution in Lake Mills, Glines Canyon Project, and Lake Aldwell, Elw ha project, Washington: Boise, Idaho, Bureau of Reclamation, Elwha Technical Series PN-95-459, 61 pp.

Jimenez, J., A. Sanchez-Arcilla, H. I. Valdemoro, V. Gracia, and F. Nieto, 1997. Processes reshaping the Ebro delta, *Marine Geology*, v. 144, issues 1-3, p. 59-79.

Lesser, G.R., Roelvink, J.A., van Kester, J.A.T.M., and Stelling, G.S., 2004. Development and validation of a three-dimensional morphological model. *Coastal Engineering* v. 50, p. 883-915.

Mulder, T. and Syvitski, J.P.M., 1995. Turbidity currents generated at river mouths during exceptional discharge to the worlds oceans. *Journal of Geology*, v. 103, p. 285-298.

Randle, T. J., C. A. Young, J. T. Melena, and E. M. Ouellette, 1996. Sediment analysis and modeling of the river erosion alternative. Elwha Technical Series PN-95-9, U.S. DOI, Bureau of Reclamation, Boise, ID.

Schwartz, M. and Johannessen, J., 1997. Historical shoreline change at the Elwha River delta shore. Consulting report prepared for the Elwha S'Klallam Tribe, Coastal Consultants, Inc. Bellingham, WA. 24 p.

Signell, R.P. and Harris, C.K., 2000. Modeling sand bank formation around tidal headlands, *in Estuarine and Coastal Modeling,* 6th Int. Conference, ASCE, New Orleans, LA. Editors: Malcolm Spaulding and Alan Blumberg.

van Rijn, L.C., 1993. Principles of sediment transport in rivers, estuaries, and coastal seas. Aqua Publications, Amsterdam.

van Wellen E., Chadwick, A.J., and Mason, T., 2000. A review and assessment of longshore sediment transport equations for coarse-grained beaches. *Coastal Engineering*, v. 40, p. 243-275.

Wallace, R.S., 1988. Quantification of net shore drift rates in Puget Sound and the Strait of Juan de Fuca, Washington. *Journal of Coastal Research*, v. 4, sect. 3, p. 395-403.

Walstra, D.J., Roelvink, J.A., and Groeneweg, J, 2000. Calculations of wave-driven currents in a 3D mean flow model. *Proceedings of 27th Conference on Coastal Engineering*, p. 1050-1063.

Warrick, J.A., Cochrane, G.R., Sagy, Y., and Gelfenbaum, G., 2008. Nearshore substrate and morphology offshore of the Elwha River, Washington. *Northwest Science*, v. 82, p.153-163.

Warrick, J.A., George, D.A., Gelfenbaum, G., Ruggiero, P., Kaminsky, G. M., and Beirne, M., in press. Beach morphology and change along the mixed grain-size delta of the dammed Elwha River, Washington. *Geomorphology*, 33 pages. doi:10.1016/j.geomorph.2009.04.012.

Warrick, J.A., George, D.A., Stevens, A.W., Eshleman, J., Gelfenbaum, G., Kaminsky, G. M., Schwartz, A.K., and Bierne, M., 2007, Beach morphology monitoring in the Elwha River littoral cell, 2004-2006: U.S. Geological Survey, Data Series 288, 38 p.